Journal of Nano- and Electronic Physics
Vol. **14** No 5, 05013(6pp) (2022)

Журнал нано- та електронної фізики
Том **14** № 5, 05013(6cc) (2022)

Super-Hydrophobic F-Doped SnO_2 (FTO) Nanoflowers Deposited by Spray Pyrolysis Process for Solar Cell Applications

Noubeil Guermat[1,*], Warda Darenfad[2], Kamel Mirouh[2], Mehdi Kalfallah[1], Mehdi Ghoumazi[3]

[1] *Department of Electronics, Faculty of Technology, University Mohamed Boudiaf of M'sila, 28000 M'sila, Algeria*
[2] *Thin Films and Interfaces Laboratory (LCMI), University of Constantine 1, 25000 Constantine, Algeria*
[3] *Research Unit in Optics and Photonics (UROP), Center for the Development of Advanced Technologies (CDTA), University of Setif-1, 19000 Setif, Algeria*

(Received 16 May 2022; revised manuscript received 19 October 2022; published online 28 October 2022)

Polycrystalline films of undoped and fluorine-doped SnO_2 (FTO) are deposited on a glass substrate by spray pyrolysis at 400 °C. The effects of fluor concentration (8, 10 and 12 %) on the structural, morphological, optical and electrical properties of FTO films are studied. Our XRD results show that F-SnO_2 still has the same rutile structure as undoped SnO_2 with improved crystallization for doped films, with no other phase detected. The measured contact angles are < 90° for undoped and 8 % F doped films, which confirms the hydrophilic character, while other doped (SnO_2:10 % F and SnO_2:12 % F) films show the hydrophobic character at contact angle values of > 90° and the super-hydrophobic (CA = 140°) for SnO_2:12 % F thin film. A higher transmittance value of 83 %, a wide band gap equal to 3.9 eV, and lower disorder (287.68 meV) are observed for the 12 % F doped SnO_2 film. In addition, electrical resistivity (ρ), carrier concentration (n) and Hall mobility (μ) are determined from Hall effect measurements and it is found that all the elaborated thin films have n-type conductivity. The lowest resistivity of 2.245×10^{-4} Ω·cm and the highest Hall mobility of 24.55 $cm^2 \cdot V^{-1} \cdot s^{-1}$ are obtained at an F concentration of 12 %. The results suggest that the FTO film at 12 %F can be used as a transparent conductive oxide of the front electrode for film solar cells.

Keywords: Thin films, F-doped SnO_2, Spray pyrolysis, Contact angle, Super-hydrophobic.

DOI: 10.21272/jnep.14(5).05013 PACS number: 82.30.Lp

1. INTRODUCTION

In recent years, significant efforts by several researchers have been focused on the development of thin films of transparent conductive oxides (TCOs) at a lower cost. Three materials are featured: tin-doped indium oxide (In_2O_3:Sn or ITO) [1], aluminum-doped zinc oxide (ZnO:Al) [2], and fluorine-doped tin oxide (SnO_2:F or abbreviated as FTO) [3] or antimony (SnO_2:Sb) [4]. These oxides have three main characteristics in common: (i) the width of the optical gap is > 3 eV, (ii) the stoichiometric compound is an insulator, and (iii) the degenerate material has a high carrier density. Tin dioxide (SnO_2) is one of the most widely used TCOs in technology. Indeed, in recent decades it has experienced increasing scientific and industrial interest in the form of thin layers due to its remarkable physical properties, more particularly its n-type semiconductor character and its good optical transparency in the visible range. These properties also make this material an ideal candidate for several practical applications such as gas sensors [5], photovoltaic cells [6], photocatalysis and others. The physico-chemical properties of thin layers of tin oxide depend on the process used for the deposition and conditions of elaboration. To produce high quality SnO_2 thin films, characterized by high optical transparency and strong electrical conduction, and with a reduced manufacturing cost, particular attention is paid above all to the manufacturing conditions, the effects of the nature of the substrates, and atomic doping (Ni, Co, Mn, Mg, Al, F, …). Several known methods are commonly used to prepare SnO_2 thin films. These are physical and chemical deposition methods. Among the methods for producing thin layers of tin dioxide, our choice fell on the spray pyrolysis process. The many advantages offered by this process (simplicity, lower cost and good homogeneity of the films produced) [5-8] justify the choice of this method.

Despite a very large number of studies on fluorine-doped SnO_2-based solar cells, the effect of this addition has so far remained poorly understood. In this context, this work focuses, on the one hand, on the production of thin layers of tin dioxide SnO_2 using the spray pyrolysis method and, on the other hand, on the study of the influence of doping atoms with fluorine (F), as a physical parameter, on the physical properties of our films, in order to obtain layers of good structural, morphological, optical and electrical quality.

2. EXPERIMENTAL DETAILS

We used as a source of tin (SnO_2) chloride dihydrate ($SnCl_2$ $2H_2O$) and a source of fluor (F) NH_4F with molarity fixed at 0.1 M. Both sources were dissolved in 20 ml of distilled water, then the obtained mixture was stirred at 30 °C for 1 h to obtain a homogeneous and transparent solution. Four undoped samples, SnO_2, SnO_2:8 %F, SnO_2:10 %F and SnO_2:12%F, were elaborated using the spray pyrolysis method on ordinary glass substrates with a deposition time of 10 min, a distance between atomizer and substrate = 17 cm and a substrate temperature of 400 °C. Structural properties were determined by XRD using a Philips X' Pert system with CuKα radiation ($\lambda_{CuK\alpha}$ = 1.5418 Å). The surface morphology and microstructure were investigated by scanning electron microscope (SEM) embedded with

* noubeil.guermat@univ-msila.dz

an Energy Dispersive X-ray (EDS) system (FEI Quanta 450 FEG). The values of the contact angle for each deposit were obtained after 5 s with a drop of distilled water of volume = 5 µl. The optical transmission measurements were carried out using a Shimadzu UV-3101 PC spectrophotometer in a range between 300 nm and 800 nm. The electrical properties (resistivity, molarity and density) were characterized at room temperature by the Hall effect method.

3. RESULTS AND DISCUSSION

The crystal structure was determined by XRD of SnO_2 and SnO_2:F thin films deposited by spray pyrolysis with different concentrations of fluorine doping (8, 10, and 12 %) at 400 °C (see Fig. 1). The results clearly indicate that all the films are of a tetragonal rutile structure with a polycrystalline nature compared to the JCPD reference files (sheet N°41-1445) [5, 6]. The major peaks are located at 26.98°, 34.19°, 38.47°, 52.04°, 62.14° and 65.98° corresponding to (110), (101), (200), (211), (310) and (301) diffraction planes, respectively. A strong orientation (110) is observed at 0 and 8 % which indicates that the films have a strong crystallographic texture according to (110), where the formation energy is lower [3]. Above these values at 10 % and 12 %, we can see that the orientation has been changed to (200), which has high texture growth [3]. As the fluorine doping concentration increases, the structure of rutile remains the same. Other main cassiterite planes were also detected but with significantly lower intensities. It appears from the XRD spectra that no peak of the impurity phase originating from the F dopant or its oxide is detected in the prepared samples. This is easily explained by the strong dilution of fluor in the structure of SnO_2 by replacing O atoms with F atoms in F-SnO_2 films [9]. The same result was observed by Khelifi et al. [3] by studying SnO_2:F films deposited by ultrasonic spray for fluorine concentrations varying between 2 and 5 % and a substrate temperature equal to 450 °C.

The crystallites size (D) of the (110) peak was calculated from the Debye-Scherrer formula [10, 11]:

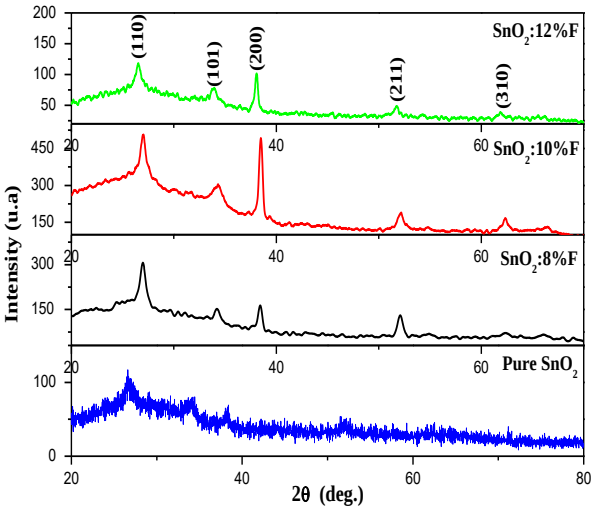

Fig. 1 – X-ray diffraction spectra of obtained films with different doping concentrations

$$D = \frac{0.9\lambda}{\beta \cos\theta}, \quad (1)$$

where λ is the wavelength of X-rays radiation, β represents the full width at half maximum (FWHM) and θ is the angle of diffraction.

The dislocation density (δ) of SnO_2 film along the (110) plane is calculated by the following formula [10]:

$$\delta = \frac{1}{D^2}. \quad (2)$$

Table 1 summarizes values of the FWHM, crystallite size and dislocation density of various undoped and SnO_2 doped layers depending on the concentration of the dopant F.

Table 1 – Variation of the FWHM, crystallites size and dislocation of our films

Sample type	FWHM	D, nm	$\delta \times 10^{-3}$, nm^{-2}
Undoped SnO_2	0.53777	15.189	4.334
SnO_2:8 % F	0.48347	16.907	3.498
SnO_2:10 % F	0.37513	21.767	2.110
SnO_2:12 % F	0.51684	15.802	4.004

The values of the crystallite size, FWHM and dislocation as a function of fluorine doping concentration are summarized in Table 1. We notice that the crystallite size values increase from 15.189 nm in the case of the undoped film to 21.767 nm at 10 % dopant concentration, while dislocations decrease due to the substitution of O atoms by F atoms in the F-SnO_2 lattice [9]. According to Bouhdjer et al. [12], this increase is probably due to an increase in the number of fluorine atoms entering the substrate, which have a large atomic radius, resulting in an increase in the nucleation number that combine to form larger grains. Beyond 10 %F, the size of crystallites decreases (15.802 nm) probably due to the incorporation of F ions in the SnO_2 network which takes interstitial sites [3].

The surface morphology and structure of the films were studied using SEM observations. In Fig. 2a, the surface of the undoped SnO_2 film has a rough appearance. It is formed of irregular agglomeration of grains with the appearance of a cubic phase.

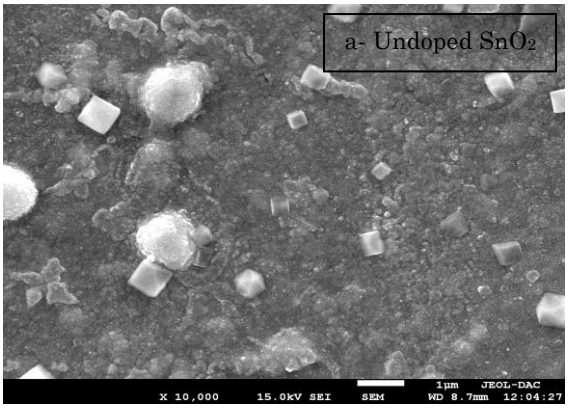

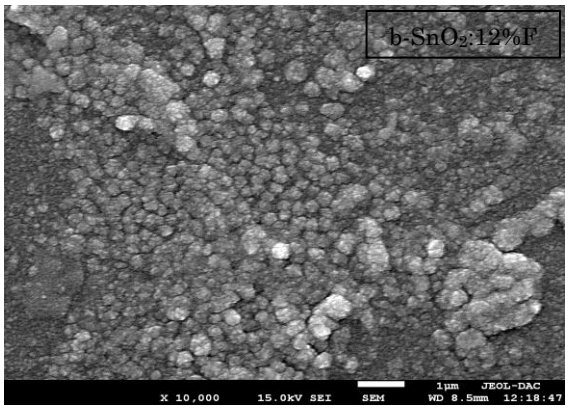

Fig. 2 – Scanning electron micrographs of a) pure and b) SnO_2: 12 % F thin films

Fig. 2b illustrates that the surface of the film is uniform and consists of crystalline nanoflowers (as shown by magnification), compact and dense. The crystalline nanofluors are smoothly distributed on the glass substrate with strong adhesion and without macroscopic defects such as voids and cracks. We also observed the disappearance of the SnO_2 cubic phase.

The EDS spectra of the deposited undoped and F-doped SnO_2 (FTO) films are shown in Fig. 3. The analysis indicates the presence of Sn,O and F elements forming the layer of undoped SnO_2 and F-doped SnO_2.

Fig. 4 shows the different static images of our films of a drop of water with a volume of 5 µl and 5 s (to avoid any effect of liquid water evaporation).

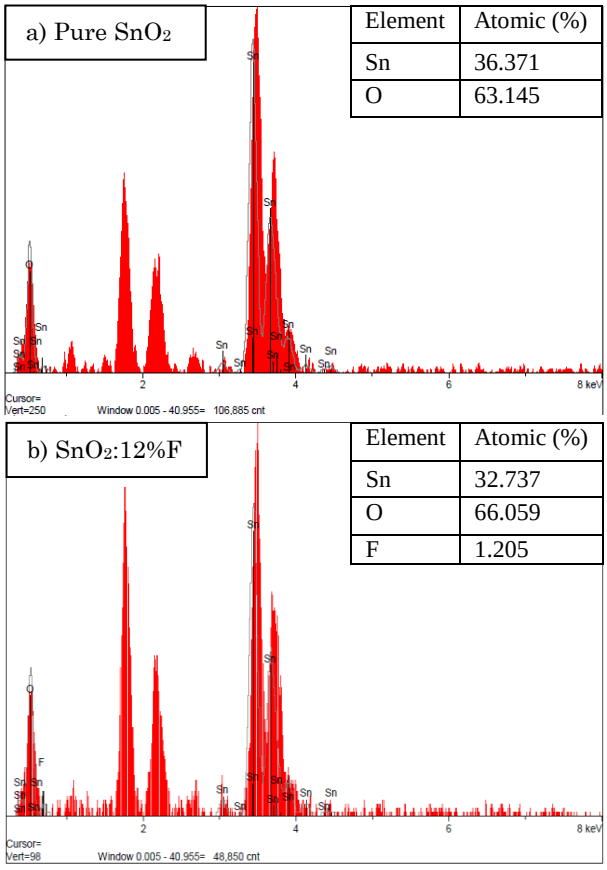

Fig. 3 – EDX spectrum of pure and SnO_2:12 % F thin films

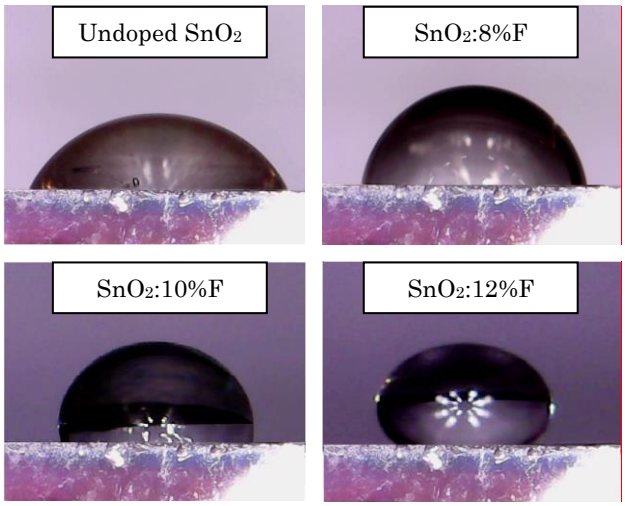

Fig. 4 – Water CA of our films

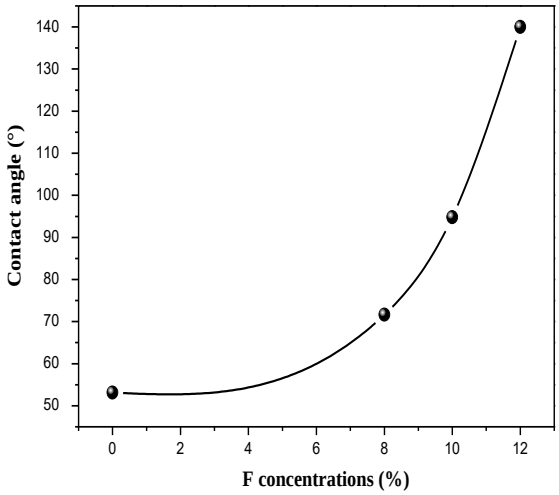

Fig. 5 – Variation of water CA of SnO_2 films at various F concentrations

Fig. 5 shows the variation of the contact angle (CA) with a drop of water of the undoped and F-doped SnO_2 films. From Fig. 4, we can see an increase in CA depending on the addition of F from 51 up 140°. The same result was observed by Ben Ameur et al. [13] by studying undoped and F-doped SnO_2 films deposited by the spray pyrolysis technique. For undoped and 8 % F doped films, the values of CA are < 90°, which describes the hydrophilic character. This behavior is similar to the results reported in the literature, such as Ni-doped SnO_2 [5] and Zn-doped SnO_2 thin films [6]. This character presents a promising feature for photocatalytic [7] and gas sensor [3, 14, 15] applications. This behavior could be attributed to the effect of layer density, surface roughness and dopant level. Beyond 8 %, the CA values measured are > 90°, which shows the hydrophobic nature of the films produced by the spray pyrolysis method. This character presents an important characteristic for solar cells.

The optical transmittance spectra are illustrated in Fig. 6. All spectra show high transparency in the visible range (400-800 nm) with an average transmittance of approximately 75 % for each film.

Interference fringes can be observed for all samples; this observation confirms the homogeneity of the elaborated layers. Moreover, we can easily notice that the doping of SnO_2 by fluorine leads to an improvement in optical transmission. The high optical transmission (T = 83 %) for the 12 % F doped film suggests that this film can be used as a window layer in thin film solar cells and in different optoelectronic devices like in flat plate collectors.

To better see the effect of doping on the behavior of SnO_2-based films produced by spray pyrolysis, we have carried out an enlargement of the transmission slices at the level of the fundamental absorption zone in the UV region for lengths ≤ 400 nm, as shown in Fig. 7. For a wavelength equal to 400 nm, it can be seen that transmittance diagrams clearly evoke the drop due to inter-band absorption (fundamental absorption). A shift towards shorter wavelengths for undoped and F-doped films, which reflects the Burstein-Moss (BM) effect [16] and results in enhanced transmission in the UV range, is a very important feature for thin-film solar cell applications, as they allow more high-energy photons to reach the solar cell.

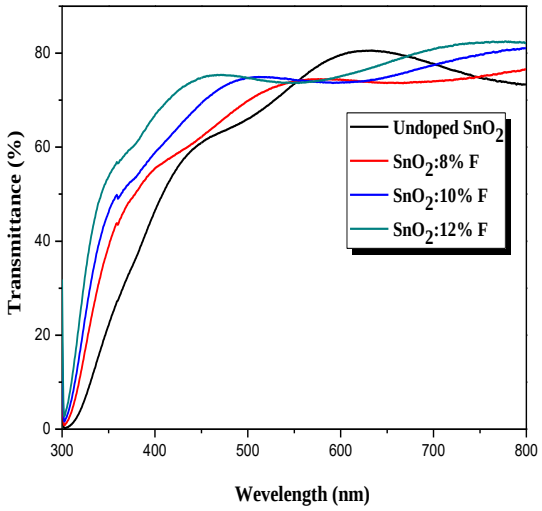

Fig. 6 – Transmission spectra of ZnO thin films deposited with different F doping concentrations

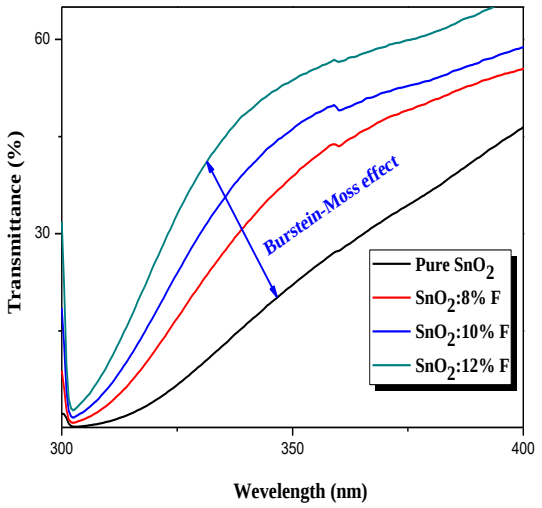

Fig. 7 – Zoom of the transmittance spectra for λ = 400 nm of our films

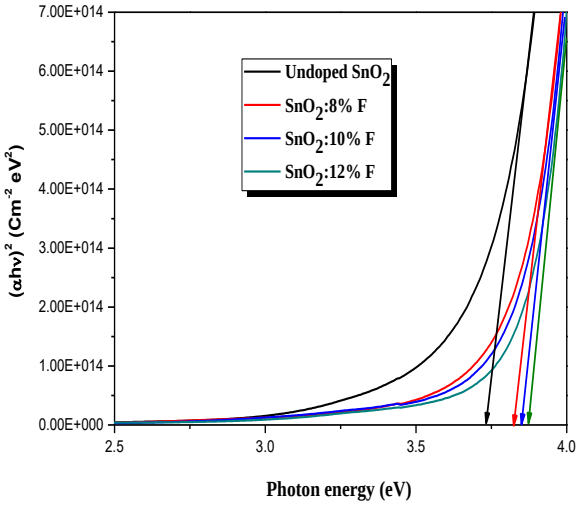

Fig. 8 – Determination of the gap energy of SnO_2 layers produced by spray pyrolysis with deferent fluoride doping

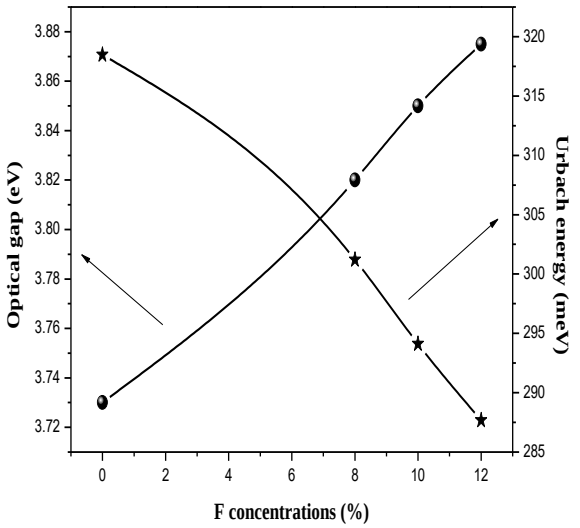

Fig. 9 – Variation of optical parameters of SnO_2 films at various F concentrations

The direct optical gap (E_g) for undoped and F-doped SnO_2 films is estimated from plots of $(\alpha h\nu)^2$ vs. photon energy ($h\nu$), as shown in Fig. 8, using Tauc's equation [17]. Fig. 8 gives an illustration of the determination of E_g of SnO_2 thin films as a function of doping rate. The determination of the optical gap of the films is deduced by extrapolation of the linear part to the $h\nu$ axis.

The variation of the optical gap as a function of F doping concentration is shown in Fig. 9. Fig. 9 shows that addition of dopant tends to increase the gap. This shift of the optical gap with the addition of F-doping (i.e. carrier concentration) can be explained by the BM shift; the absorption edge shifts to higher energies with increasing carrier concentration [18]. Similar behavior has been observed by several authors [3, 16, 18].

Localized states near the edge of the band can cause band tails [17]. The absorption edge is called the Urbach tail [17]. The Urbach energy (E_U) or the disorder is probably related to the effects of all possible defects. The Urbach energy is given by the following equation [17]:

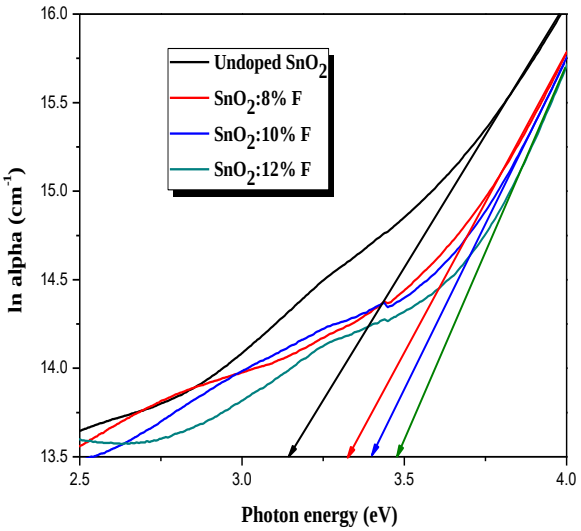

Fig. 10 – Plots of $\ln\alpha$ versus photon energy $h\nu$ for determining Urbach energy of SnO_2 thin films deposited with different F doping concentrations

$$\alpha = \alpha_0 \exp\frac{h\nu}{E_u}, \quad (3)$$

where α_0 is a constant.

The Urbach energy for SnO_2 thin films deposited with different F doping concentrations is determined by plotting $\ln\alpha$ against the energy of photons $h\nu$, as shown in Fig. 10. The Urbach energy of the undoped sample is 318 meV and this value decreases with increasing doping content. Since Urbach energy is related to structural defects, the decrease in structural defects observed from XRD analysis (Table 1) with doping leads to a decrease in the Urbach energy values.

Table 2 – Variation of resistivity (ρ), Hall mobility (μ) and carrier concentration (n) for different F doping in SnO_2 films

Sample type	ρ, Ω·cm	μ, $cm^2\ V^{-1}\ s^{-1}$	n, cm^{-3}
Pure SnO_2	3.721	3.24×10^{-3}	1.24×10^{14}
SnO_2:8 % F	1.47×10^{-1}	4.458×10^{-2}	9.494×10^{16}
SnO_2:10 % F	8.265×10^{-2}	8.756×10^{-1}	8.626×10^{19}
SnO_2:12 % F	2.245×10^{-4}	2.455×10^{1}	1.128×10^{21}

Table 2 shows the variation of Hall mobility (μ), carrier concentration (n) and resistivity (ρ) of SnO_2:F films with various F concentrations. It is observed that Hall effect measurements indicate that undoped and F-doped SnO_2 films are n-type semiconductors. An increase in the carrier concentration and Hall mobility with increasing fluorine doping can be explained by the increase in the crystallite size of the films as a function of the addition of F, as shown by the diagram of X-ray diffraction (Fig. 2). So, improving the crystallinity of films reduces carrier loss, as reported by Vasu and Subrahmanyam [19]. As a result of an increase in the carrier concentration and Hall mobility, the resistivity of these films decreases (Table 2). This can be attributed to fluorine ions occupying oxygen sites in the SnO_2 lattice creating free electrons resulting in an increase in electrical conductivity. In addition, the value of ρ (2.245×10^{-4} Ω·cm) is minimum and μ (2.455×10^{1} $cm^2\ V^{-1}\ s^{-1}$) and n (1.128×10^{20} cm^{-3}) are maximum for the 12 % F-doped film, indicating that this is the optimum concentration for optoelectronic applications.

Table 3 – Comparison of the resistivity, mobility and carrier concentration of SnO_2:F films as reported by other authors and in the present study

Method	ρ, Ω·cm	μ, $cm^2\ V^{-1}\ s^{-1}$	n, cm^{-3}	Ref.
PLD	1.3×10^{-3}	13.9	3.6×10^{20}	18
APCVD	4.99×10^{-4}	17.8	7.09×10^{20}	20
Sputtering	1.7×10^{-2}	–	–	21
Ultrasonic spray pyrolysis	8.5×10^{-4}	–	–	22
Ultrasonic spray pyrolysis	4.52×10^{-4}	24.68	5.73×10^{20}	23
Spray pyrolysis	2.3×10^{-4}	74	6.9×10^{20}	24
Spray pyrolysis	15×10^{-4}	21.86	1.87×10^{20}	25
Spray pyrolysis	2.245×10^{-4}	24.55	1.128×10^{20}	Present study

Table 3 presents the values of the electrical resistivity for thin layers of FTO deposited by different techniques. It is interesting to note that the best value of the electrical resistivity obtained in this work is lower than that obtained by spray pyrolysis, ultrasonic spray pyrolysis, pulsed laser deposition (PLD), atmosphere pressure chemical vapor deposition (APCVD) and sputtering techniques.

4. CONCLUSIONS

In summary, undoped and F-doped SnO_2 (FTO) thin films on glass substrates elaborated by the spray pyrolysis process were successfully synthesized in this study. Experimental results revealed that the deposited materials have a tetragonal rutile structure with a polycrystalline nature, and no impurity phase is observed. The undoped and 8 % F doped SnO_2 films show a hydrophilic character with CA < 90° and other elaborate films show a hydrophobic character (CA > 90°) and a super-hydrophobic for the 12 % F doped. For a SnO_2: 12 % F film, a low electrical resistivity of 2.245×10^{-4} Ω·cm with the high optical transmission of 83 % in the visible spectral range was measured and compared to other elaborated films. We deduced that doping with 12 %F is an optimal value for the FTO film deposited by the spray pyrolysis technique, which gives the best structural, morphological, super-hydrophobic, optical and electrical properties required as a conductive transparent electrode in solar cell thin layers.

ACKNOWLEDGEMENTS

This work is supported by the Research Project University Formation (PRFU) of Algerian ministry of high education and scientific research (No. A10N01UN280120220009) entitled 'Study, elaboration and characterization of the effect of doping and co-doping on the properties of oxides of transition metals for optoelectronic applications'.

REFERENCES

1. A. Khan, F. Rahman, R. Nongjai, K. Asokan, *Curr. Appl. Phys.* **38**, 49 (2022).
2. P. Kumar, S.M. Dharmaprakash, *Appl. Surf. Sci.* **593**, 153423 (2022).
3. Ch. Khelifi, A. Attaf, H. Saidi, A. Yahia, M. Dahnoun, *Surf. Interface.* **15**, 244 (2019).
4. J. Sawahata, M.M. Islam, *Thin Solid Films* **752**, 139249 (2022).
5. M. Khalfallah, N. Guermat, W. Daranfed, N. Bouarissa, H. Bakhti, *Phys. Scr.* **95**, 095805 (2020).
6. N. Guermat, W. Darenfad, K. Mirouh, N. Bouarissa, M. Kalfallah, A. Herbadji, *Eur. Phys. J. Appl. Phys.* **97**, 14 (2022).
7. W. Darenfad, N. Guermat, K. Mirouh, *J. Nano- Electron. Phys.* **13** No 6, 06016 (2021).
8. W. Daranfed, N. Guermat, I. Bouchama, K. Mirouh, S. Dilmi, M. A. Saeed, *J. Nano-Electron. Phys.* **11** No 6, 06001 (2019).
9. A.H. Omran Alkhayatt, S.K. Hussian, *Mater. Lett.* **155**, 109 (2015).
10. N. Guermat, W. Daranfed, I. Bouchama, N. Bouarissa, *J. Mol. Struct.* **51**, 129134 (2021).
11. N. Guermat, W. Daranfed, K. Mirouh, *Annales de Chimie - Science des Matériaux* **44**, 347 (2020).
12. A. Bouhdjer, A. Attaf, H. Saidi, H. Bendjedidi, Y. Benkhetta, I. Bouhaf, *J. Semicond.* **36**, 82002 (2015).
13. S. Ben Ameur, A. Barhoumi, H. Bel hadjltaief, R. Mimouni, B. Duponchel, G. Leroy, M. Amloukc, H. Guermazi, *Mater. Sci. Semicond. Process.* **61**, 17 (2017).
14. N. Guermat, A. Bellel, S. Sahli, Y. Segui, P. Raynaud, *Defect Diffusion Forum.* **354**, 41 (2014).
15. N. Guermat, A. Bellel, S. Sahli, Y. Segui, P. Raynaud, *Thin Solid Films* **517**, 4455 (2009).
16. Anusha, B.S. Acharya, A. Antony, A. Ani, I.V. Kityk, J. Jedryka, P. Rakusb, A. Wojciechowski, P. Poornesh, S.D. Kulkarni, *Opt. Laser Technol.* **119**, 105636 (2019).
17. W. Daranfed, N. Guermat, K. Mirouh, *Annales de Chimie - Science des Matériaux* **44**, 121 (2020).
18. H. Kim, R.C.Y. Auyeung, A. Piqué, *Thin Solid Films* **520**, 497 (2011).
19. V. Vasu, A. Subrahmanyam, *Thin Solid Films* **189**, 217 (1990).
20. H.L. Ma, D.H. Zhang, S.Z. Win, S.Y. Li, Y.P. Chen, *Sol. Energy Mater. Sol. Cells.* **40**, 371 (1996).
21. B.L. Zhu, F. Liu, K. Li, K. Lv, J. Wu, Z.H. Gan, J. Liu, D.W. Zeng, C.S. Xie, *Ceram. Int.* **43**, 10288 (2017).
22. E. Sakai, N. Tsutsumi, K. Horib, H. Kumigashir, Y. Tsuji, *J. Electron Spectrosc. Rel. Phenom.* **247**, 147041 (2021).
23. M.H. Jo, B.R. Koo, H.J. Ahn, *Ceram. Int.* **46**, 25066 (2020).
24. M. Thirumoorthi, J. Thomas Joseph Prakash, *Superlattice. Microstruct.* **89**, 378 (2016).
25. K.K. Purushothaman, M. Dhanashankar, G. Muralidharan, *Curr. Appl. Phys.* **9**, 67 (2009).

Леговані фтором супергідрофобні наноквіти SnO_2 (FTO), осаджені за допомогою розпилювального піролізу для застосування в сонячних елементах

Noubeil Guermat[1], Warda Darenfad[2], Kamel Mirouh[2], Mehdi Kalfallah[1], Mehdi Ghoumazi[3]

[1] *Department of Electronics, Faculty of Technology, University Mohamed Boudiaf of M'sila, 28000 M'sila, Algeria*
[2] *Thin Films and Interfaces Laboratory (LCMI), University of Constantine 1, 25000 Constantine, Algeria*
[3] *Research Unit in Optics and Photonics (UROP), Center for the Development of Advanced Technologies (CDTA), University of Setif-1, 19000 Setif, Algeria*

Полікристалічні плівки нелегованого та легованого фтором SnO_2 (FTO) наносяться на скляну підкладку методом розпилювального піролізу при 400 °C. Досліджено вплив концентрації фтору (8, 10 і 12 %) на структурні, морфологічні, оптичні та електричні властивості плівок FTO. Наші результати XRD показують, що F-SnO_2 все ще має ту саму структуру рутилу, що й нелегований SnO_2, з покращеною кристалізацією для легованих плівок та без виявлення іншої фази. Виміряні кути контакту становлять < 90° для нелегованих плівок та плівок, легованих 8 % F, що підтверджує гідрофільний характер, тоді як інші леговані плівки (SnO_2:10 % F і SnO_2:12 % F) демонструють гідрофобний характер при значеннях кута контакту > 90° та супергідрофобний характер (CA = 140°) для тонкої плівки SnO_2:12 % F. Для плівки SnO_2, легованої 12 % F, спостерігається вищий коефіцієнт пропускання 83 %, ширина забороненої зони 3,9 еВ і менший безлад (287,68 меВ). Крім того, питомий електричний опір (ρ), концентрація носіїв (n) і холлівська рухливість (μ) визначаються за допомогою вимірювань ефекту Холла, і виявлено, що всі розроблені тонкі плівки мають n-тип провідності. Найнижчий питомий опір $2{,}245 \times 10^{-4}$ Ом·см і найвища холлівська рухливість 24.55 $см^2 \cdot В^{-1} \cdot с^{-1}$ отримані при концентрації 12 % F. Результати свідчать про те, що плівку FTO з 12 % F можна використовувати як прозорий провідний оксидний фронтального електроду для плівкових сонячних елементів.

Ключові слова: Тонкі плівки, Легований фтором SnO_2, Розпилювальний піроліз, Контактний кут, Супергідрофобний.